Please cite this article at: Mahdi Sharifzadeh Mojtaba Meghdari, Davood Rashtchian. Multi-objective design and operation of Solid Oxide Fuel Cell (SOFC) Triple Combined-cycle Power Generation systems: Integrating energy efficiency and operational safety. Applied Energy, 185 (1), 345-361.

Multi-objective Design and Operation of Solid Oxide Fuel Cell (SOFC) Triple Combined-cycle Power Generation Systems: Integrating Energy Efficiency and Operational Safety

Mahdi Sharifzadeh [a] [1], Mojtaba Meghdari [b], Davood Rashtchian [b]

[a] Centre for Process System Engineering (CPSE), Department of Chemical Engineering, Imperial College London, SW7 2AZ, UK.

[b] Department of Chemical and Petroleum Engineering, Sharif University of Technology, Tehran, Iran.

Abstract

Energy efficiency is one of the main pathways for energy security and environmental protection. In fact, the International Energy Agency asserts that without energy efficiency, 70% of targeted emission reductions are not achievable. Despite this clarity, enhancing the energy efficiency introduce significant challenge toward process operation. The reason is that the methods applied for energy-saving pose the process operation at the intersection of safety constraints. The present research aims at uncovering the trade-off between safe operation and energy efficiency; an optimization framework is developed that ensures process safety and simultaneously optimizes energy-efficiency, quantified in economic terms. The developed optimization framework is demonstrated for a solid oxide fuel cell (SOFC) power generation system. The significance of this industrial application is that SOFC power plants apply a highly degree of process integration resulting in very narrow operating windows. However, they are subject to significant uncertainties in power demand. The results demonstrate a strong trade-off between the competing objectives. It was observed that highly energy-efficient designs feature a very narrow operating window and limited flexibility. For instance, expanding the safe operating window by 100% will incur almost 47% more annualized costs. Establishing such a trade-off is essential for realizing energy-saving.

Keywords

Integrated Process Design and Control, Safe Process Operation, Multi-objective Optimization under Uncertainty, SOFC Triple Combined-cycle Power Generation Systems.

[1] **Corresponding author:** Dr Mahdi Sharifzadeh; Room C603, Roderic Hill Building, South Kensington Campus, Imperial College London, UK. SW7 2AZ. E-mail: mahdi@imperial.ac.uk ; Tel: +44 (0)75 1785 3422, Fax: +44 (0)20 7594 6621

1. Introduction

Fuel Cells are very promising energy conversion technologies that can oxidize the fuel electrochemically and avoid the exergy destructions associated with combustion. Furthermore, they are highly modular and can be applied for a very wide range of power demands. Amongst various fuel cell technologies, solid oxide fuel cells (SOFCs) has the advantage of operating at very high temperature (>1000 C) and potential integration with downstream Rankine and/or Brayton Cycles [1]. Triple Combined-cycle Power Generation Systems, also known as hybrid SOFC power plants, refer to the energy conversion processes in which solid oxide fuel cells (SOFCs) are integrated with a gas turbine followed by heat recovery and steam generation. Due to inclusion of the SOFCs, Triple Combined-cycle Power Generation System feature significantly higher conversion efficiency (>75%, [2,3]) compared to conventional combined cycle power plants (<50% [4,5]). Furthermore, these generation systems are proved to be highly adaptive to various feedstocks [6–10]. They can be also integrated with the gas and steam turbines directly, indirectly or via fuel coupling. This combination of merits has made SOFC Triple-cycle Power Generation systems very attractive and the focus of various academic and industrial research. Andersson et al [11] reviewed various approaches that were applied for modeling Fuel Cells. They concluded that accurate prediction of fuel cell operation would require multi-scale modeling and capturing the complex interactions between mass, heat and momentum transfer phenomena. Zhao, et al [12] studied the efficiency of hybrid SOFC-GT systems using optimization programming. They concluded that the highest energy efficiency requires the largest temperature ratio over the gas-turbine. Calise, et al [13] studied the full-load and part-load operation of Hybrid SOFC power plants using exergy analysis. They concluded that the most efficient part load operation can be achieved by maintaining the ratio of combustion air to fuel constant, [14,15]. However, Arsalis [16] explained that such strategy can be applied only for a limited operating window (>80% electricity load). Zaccaria, et al [17] applied a cyber-physical system and step changes to identify the transfer function model, which was applied for characterization of the system dynamic response. They identified the cold air bypass valve as a critical manipulated variable that can efficiently control compressor surge in SOFC/GT hybrid systems. Harun, et al [18] emphasized on the flexibility of the SOFC hybrid power plants for handling variable fuel compositions. They characterized the spatial variations of the fuel composition, as well as thermal, and electrochemical performances across the SOFC. Fardadi, et al [19] proposed a multi-input multi-output controller in order to suppress the spatial temperature variations during power load fluctuations. They emphasized on simultaneous consideration of process design and control for safe thermal operation. Facci, et al [20] studied a small-scale tri-generation system applied for cooling, heating and power generation in a residential area. They studied two scenarios in which the economy and primary energy consumptions were optimized, respectively. They concluded that the choice of the objective affects the optimal design and control strategies.

The abovementioned studies illustrate the merits as well as complexities of hybrid SOFC power generation systems. Due to existence of three power generation cycles (i.e., SOFC syngas cycle, gas turbine cycle, and steam turbine cycle), the operation of SOFC power plants is highly constrained by various technical and safety criteria. As the direct result of high degree of energy and mass integration, disturbances and fluctuations propagate in various pathways resulting in much narrower operating window compared to conventional power generation systems. Nonetheless, power plants are subject to large uncertainties in electricity demand and require flexible operation. In the future, by introduction of renewable energies such as wind and solar, power plants need to operate even more flexibly to balance out the intermittent power generation from these new members of the electricity grid. Therefore, commercialization of SOFC Triple Combined-cycle Power Generation Systems strongly depends on their ability to operate safely and flexibly. In the present paper, firstly, we review the method for safe design and operation of industrial processes. These discussions enable proposition of a new methodology that establishes a trade-off between energy efficiency and operational safety of industrial processes. Then, the problem is formulated for the challenging case of SOFC Triple Combined-cycle Power Generation Systems. The features of the developed optimization program including objective function, optimization variables and constraints are discussed. The discussions continue with explaining the modelling assumptions and implementation techniques. Later on, the optimization results are presented and discussed. Of particular interest is the trade-off between the economic and safety objectives that is illustrated using Pareto front diagrams in terms of the required capital investment and operating costs. Other features of interest include investigating the implications of electricity load reduction for process safety and energetic performance using computational fluid dynamic simulations and exergetic analysis. The paper concludes with summarizing the research finding and suggesting future research directions.

2. Methodology and background

Process industries are associated with hazardous chemicals and extreme operating conditions. Unsafe events can result in dramatic consequences in terms of the loss of life, the loss of capital and environmental damages. Therefore, safety measures must be considered at the same level of profitability and production costs [21]. Early stage research in the field of operational safety advocated qualitative techniques for hazard identification. Examples of qualitative techniques include application of engineering insights in terms of checklists [22–25]. Alternatively, preliminary hazard analysis (PHA) is a causal technique that identifies the sequences of events leading to an accident [26–29]. More comprehensive analysis would require process and instrumentation diagrams (P&ID) and teamwork in terms of hazard and operability (HAZOP) studies.

The limitation of the qualitative techniques is their dependence on the experience and knowledge of practitioners. Furthermore, the estimation methods apply relative measures such as “low”, “high”, “more”, or “less”, which make the results to large extent subjective. By comparison, quantitative methods such as quantitative risk assessment (QRA) and probabilistic safety assessment (PSA) apply indices which enable comparisons of various decisions. Examples of quantitative measures include (Dow’s Fire & Explosion Index (F&EI) [30], Inherent Safety Index (ISI) [31], Process Route Index (PRI) [32] which are applied for ranking alternative designs for reaction routes[33,34], separation technologies [24,35–37] and process layouts [38,39]. Often steady-state [40,41] or dynamic simulations [42–44] are the methods of choice. For instance, Maria and Stefan [45] studied a fixed-bed catalytic reactor. They applied a model-based global sensitivity criterion to identify the limits of safe operating conditions when there is a risk of runaway reactions. They observed that the most economic operating condition is in the vicinity of safety limits. Srinivasan and Nhan [33] emphasized on the significance of choosing inherently safer chemical process routes for eliminating or mitigating various risks and hazards. They proposed a quantitative method for process benign-ness based on various indicators such as temperature, pressure, and the properties of the involved materials. Tugnoli, et al. [38,39] proposed a Domino Hazard Index in order to enhance inherent safety of the plant layout. Domenico, et al. [40] applied UNISIM DESIGN and the PHAST software tools for assessing the acceptability of a new methanol technology. The results were presented in terms of individual and social risks. Koc, et al. [41] studied process intensification through integration of a water-gas-shift membrane reactor (WGSMR) into an Integrated Gasification Combined Cycle (IGCC) process, with the advantage of carbon capture from the retentate stream. Using Monte Carlo simulation and model-based analysis, they investigated the implications of various technological, regulatory and market uncertainties for the overall net present value (NPV). They argued that investing in safety amongst other capital expenditures, will enhance economic performance in the presence of irreducible uncertainties.

Steady-state simulations provide an understanding of process behavior in dangerous situations and the associated consequences. However, more detailed analysis requires dynamic simulations with the advantages of predicting transient process behaviors (e.g., violating path constraints) under upset operating conditions, in addition to the time window available for reverting and preventing unsafe events. Meel and Seider [42] applied a variety of loss prevention techniques in combination with dynamic simulation to quantify the frequency of abnormal events, failure probability and the proximity of the process state to accidents. They emphasized on the application of plant-specific probabilities rather than generic values. Podofillini and Dang [43] compared conventional methods (PSA and QRA) with dynamic simulation. They concluded that obtaining consistent results from conventional methods would require a large number of simulations. Nevertheless, dynamic simulations can be used to train the operators. For example, Yang et al. [44] reported the development and application of the dynamic simulation of an MTBE process for training plant operators. While dynamic simulation has been widely applied for validation and training, the scope for dynamic optimization is much more limited. The two programming approaches are hybrid state-transition [46] and region-transition models [23,47]. These methods focus either on *reachability* of unsafe conditions from a set of initial conditions or identification of the *worst-case trajectory* toward unsafe conditions. The underlying mathematical formulations consist of differential algebraic equations (DEAs), combined with binary or Boolean variables, which represent various operational modes or procedures. Uncertainties are either presented using probability distribution functions or bounds on the uncertain parameters. The limitation of these methods is the high computational costs of solving mixed-integer dynamic optimization (MIDO) problems. Furthermore, as discussed by Uygun et al, [48], identification of worst scenario requires global optimization of nonlinear dynamic models. However, the applied linearized models are only valid locally and around nominal operating points, and therefore, are incapable of predicting extreme conditions. Overall, large-scale dynamic optimization is a tough challenge for current optimization technology and the application of dynamic methods is limited to small cases. Steady-state multi-objective optimization programming provides the option for considering economic and safety objectives at the same level. The results of multi-objective optimization form a set of optimal solutions, known as a Pareto front, which demonstrates the trade-off between the competing profitability and safe operation objectives. Eini et al. [49] proposed a multi-objective optimization framework is proposed in which the safety criteria are quantified based on consequence modeling and aggregated with the economic performance using multi-objective optimization programming. Shah, et al. [50] quantified the trade-off between energy-efficiency and inherent process safety for the case of an LNG process using multi-objective optimization. Reducing hydrocarbon inventory was selected as the safety objective. El-Halwagi, et al. [51] studied a biorefinery supply chain. They demonstrated the conflicts between the economic and safety objectives in the form of Pareto fronts. While an exhaustive review of the research in the field is not in the scope of the present study, several important conclusions can be drawn from the above critical analyses:

1) Design and operation of industrial processes are highly tangled. If the process is poorly designed, ensuring safe operation, if not impossible, will incur costly modifications. Therefore, it is highly recommended that process economy and safety measures should be considered at the same level and during the early stages of process design.
2) It is widely observed that the safety and energy efficiency are competing and conflicting. Such a trade-off can be quantified in the form of Pareto fronts using multi-objective optimization (MO).
3) While optimization programming provides a systematic framework for generating alternative design solutions and screening them based on rigorous measures, there is a major barrier. During the early stage of process design, often only very limited amount of information is available. Therefore, integrating design and operation of industrial processes is not realistic without considering uncertainties.

Despite these strong incentives, currently no systematic framework exists that considers the abovementioned criteria simultaneously. The present research addresses this gap by proposing a novel optimization framework based on multi-objective optimization under uncertainty in which design and operation of industrial processes are considered at the same level. The proposed framework is demonstrated on the challenging case of an SOFC Triple-cycle Power Generation System.

2.1. A novel framework for Integrated Safe Design and Operation of industrial processes

Design and operation of industrial processes are highly tangled. If a process is poorly designed, there will be only limited and costly options left to ensure its safe and economic operation. Therefore, many commentators suggested that process design and operation should be considered simultaneously, known as integrated process design and operation, [52]. Recently, Sharifzadeh, et al. [53–55] proposed a methodology for integrated design and control of industrial processes. Their proposed framework is based on the notion of perfect control and the property that inverse solution of the process model can be applied in order to estimate the best achievable control performance. The proposed method can be applied in both steady-state and dynamic formulations and will ensure desirable properties such as self-optimizing control, functional controllability, steady-state operability and computational complexity reductions, [54,55]. While perfect control provides an upper bound on the operational performance, it is also pertinent to enquire about the lower bound. Of course, the lower bound of control performance can be detrimental, but here we focus on the least acceptable control performance. More specifically we investigate the operational range over which process constraints in terms of specification of products, environmental concerns and safety limits can be satisfied. Hereafter, we refer to this operating regions as the safe operating window. The idea is shown in Fig. 1. The total operating window over which a manipulated variable can be actuated is shown by it lower and upper bounds. However, industrial processes are subject to a variety of uncertainties and disturbances. For each uncertain scenario, there is an optimal value (shown by the green points) for each manipulated variable that can systematically handle the disturbances and at the same time optimizes the process economy. The optimal values of a manipulated variable fall in a window (shown by green line) over which all the operational constraints are satisfied. However, there might be a range of values for a manipulated variable (red lines) over which satisfaction of constraints cannot be guaranteed. Within such an operational range, the risk of violation of process constraints exists and depends on the realization of uncertainties and disturbances, as well as the action of other manipulated variables. Therefore, the process operation could be unsafe within such ranges. The present research, aims at quantification of the unsafe operating window, and the incorporation of such

Please cite this article at: Mahdi Sharifzadeh Mojtaba Meghdari, Davood Rashtchian. Multi-objective design and operation of Solid Oxide Fuel Cell (SOFC) Triple Combined-cycle Power Generation systems: Integrating energy efficiency and operational safety. Applied Energy, 185 (1), 345-361.

knowledge into design of the process. In other words, we investigate how to design industrial processes which are more flexible and can be operated over wider safe operating regions. The research objective is to formulate an algorithm which establishes the trade-off between the process economy and safe operation. In the rest of this section, the proposed optimization framework is formulated. Then, the implication of the mathematical formulation is presented graphically. In the next section, the proposed framework will be applied to the demonstrating case of a Solid Oxide Fuel Cell (SOFC) Triple Combined-cycle Power Plant.

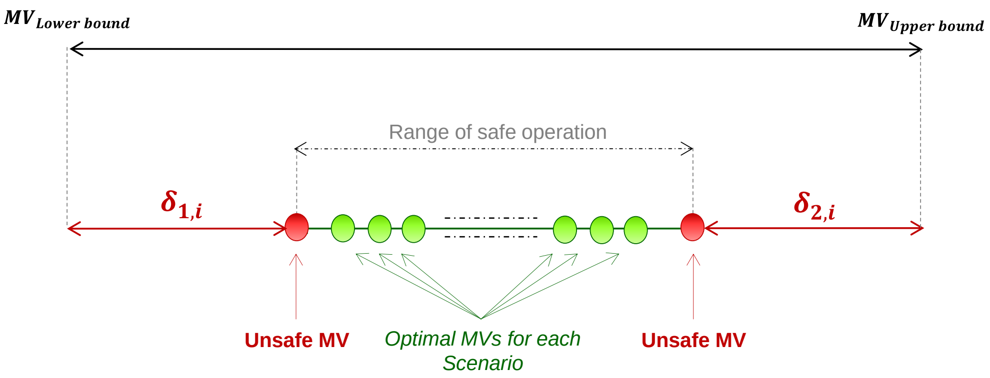

Fig. 1. Safe and unsafe operating windows

2.2. Mathematical formulation

As discussed earlier, design and operation of industrial processes have competing objectives which share their decision-making domains. In other words, highly economically competitive processes may have a limited operating window and conversely, enhancing process safety would require extra investments. Establishing such a trade-off requires *multi-objective* optimization. Here, the objective functions include economic measures as well as indicators which quantify the safe operating window. Furthermore, industrial processes are subject to various uncertainties. Examples of uncertainties include exogenous disturbances such as upset upstream conditions, in addition to uncertainties in the model parameters such as economic parameters, the rate of reactions, heat transfer coefficients, as well as measurement errors and failure of control signals. It is expected that despite all potential uncertainties, the process operation should remain safe, i.e., all the operational constraints must be satisfied. From the mathematical point of view, the formulation of the problem of integrated safe design and operation of industrial processes conforms to multi-objective optimization *under uncertainty*. To this end, we propose the following optimization formulations:

$$\min \ (E\{\boldsymbol{F}_{Economic},\}, E\{\boldsymbol{F}_{Safety}\})$$

$$s.t. \quad E\{\boldsymbol{F}_{Economic},\} = \sum_{s=1}^{n_s} L_s \times F_{economic,s}(\boldsymbol{Y_P}, \boldsymbol{p}, \boldsymbol{u}^{opt}, \boldsymbol{y}, \boldsymbol{\theta})$$

$$E\{F_{Safety}\} = \sum_{s=1}^{n_s} L_s \times F_{safety,s}(\boldsymbol{Y_P}, \boldsymbol{p}, \boldsymbol{u}^{extreme}, \boldsymbol{y}, \boldsymbol{\theta}, \boldsymbol{\delta})$$

$$\boldsymbol{h}[\boldsymbol{x}^{opt}, \boldsymbol{u}^{opt}, \boldsymbol{y}^{setpoint}, \boldsymbol{Y}_p, \boldsymbol{p}, \boldsymbol{\mu}, \boldsymbol{\theta}] = 0$$

$$\boldsymbol{g}[\boldsymbol{x}^{opt}, \boldsymbol{u}^{opt}, \boldsymbol{y}^{setpoint}, \boldsymbol{Y}_p, \boldsymbol{p}, \boldsymbol{\mu}, \boldsymbol{\theta}] \leq 0$$

$$\boldsymbol{h}[\boldsymbol{x}^{extreme}, \boldsymbol{u}^{extreme}, \boldsymbol{y}^{extreme}, \boldsymbol{Y}_p, \boldsymbol{p}, \boldsymbol{\mu}, \boldsymbol{\theta}] = 0$$

$$\boldsymbol{g}[\boldsymbol{x}^{extreme}, \boldsymbol{u}^{extreme}, \boldsymbol{y}^{extreme}, \boldsymbol{Y}_p, \boldsymbol{p}, \boldsymbol{\mu}, \boldsymbol{\theta}] \leq 0$$

$$\Omega[\boldsymbol{\mu}] = 0$$

$$\boldsymbol{\theta}^N - \boldsymbol{\sigma} \times \Delta\boldsymbol{\theta}^- \leq \boldsymbol{\theta} \leq \boldsymbol{\theta}^N + \boldsymbol{\sigma} \times \Delta\boldsymbol{\theta}^+$$

$$\boldsymbol{u}^N - \boldsymbol{\delta} \times \Delta\boldsymbol{u}^- \leq \boldsymbol{u} \leq \boldsymbol{u}^N + \boldsymbol{\delta} \times \Delta\boldsymbol{u}^+$$

$$\boldsymbol{\delta}, \boldsymbol{\sigma} \geq 0$$

$$\boldsymbol{y}^{low} \leq \boldsymbol{y}^{opt} \leq \boldsymbol{y}^{up}$$

$$\boldsymbol{y}^{extreme} \in \{\boldsymbol{y}^{low}, \boldsymbol{y}^{up}\}$$

In the above formulation, $\boldsymbol{F}_{Economic}$ represent economic objectives such as the value of products, operating costs and the required capital investment. The safety objective, $\boldsymbol{F}_{Safety}$ is the length of the operating window, over which the process operation can be guaranteed to be safe (Fig. 1). Each objective function has different values for various realizations of uncertain parameters. The expected value of the objective functions can be estimated based on the likelihood of each scenario, L_s. The equality constraints, $\boldsymbol{h}[\,]$, represent the process model. The inequalities, $\boldsymbol{g}[\,]$, include the technical constraints (e.g., product specifications). Here, we formulate the safety constraints explicitly as lower and upper bound on the controlled variables, $[\boldsymbol{y}^{lo}, \ \boldsymbol{y}^{up}]$. The justification is that important safety constraints must be either explicitly or inferentially controlled. The variables, $\boldsymbol{\mu}$, and corresponding inequalities represent the range of external disturbances or setpoint tracking scenarios. Non-negative variables, $\boldsymbol{\sigma}$ enable systematic quantification of the range of uncertain parameters. Non-negative variables $\boldsymbol{\delta}$ enable systematic quantification of the range of manipulated variables, over which safe process operation can be guaranteed (Fig. 1). We refer to such a range as the safe operating window. It should be noted that in formulation (1), there are two instances of the process model $\boldsymbol{h}[\,]$ and process constraints $\boldsymbol{g}[\,]$. In one instance, the model inversion was based on the optimal setpoints for process profitability, (i.e., green points in Fig. 1). However, it is also needed to calculate the extreme value (i.e., red points in Fig. 1) of manipulated variables in order to quantify the safe operating window. Therefore, the second model inversion is based on extreme values of the controlled variables. There are threshold values of the controlled variables beyond which process operation is considered to be unsafe. It is notable that the values of process design parameters are the same in both instances. In other words, the same model (of the same physical system) is being interrogated two times; once with respect to economically optimal design and then for quantification of the safe operating window.

2.3. Graphical representation

The aforementioned formulation can be represented using the optimization-simulation diagram shown in Fig. 2. The optimization solution algorithm is shown by the small left envelope. The large right envelope includes the constraints. The process model is inverted and interrogated two times. First, with respect to the setpoints at optimal operating conditions. Here, the optimal values of manipulated variables are shown by the green circles. Second, with respect to controlled variables at their extreme conditions in order to quantify the safe operating window. Here, the extreme values of manipulated variables beyond which safe operation cannot be guaranteed are shown by the red circles. The process model is exposed to the expected disturbance scenarios and the value of the objective function and the violation of constraints, corresponding to each disturbance scenario are calculated and sent to the optimization solution algorithm for decision-making.

It should be noted that the proposed method is different from the flexibility optimization method proposed by Grossmann and co-workers [56,57]. Flexibility optimization exploits the notion of two-stage recourse-based optimization under uncertainty. In the context of flexibility optimization, manipulated variables are available during operational phase in order to counteract the negative effects of the realization of uncertain parameters. This is not the case for the optimization of safe operating window (proposed in the present research), as in practice, the quality of control depends on the performance of the controllers. Failure in the control system for example due to the loss of control signal, measurement error or operator inappropriate intervention would result in the escalation of unsafe incidents. Therefore, it is desired to identify the range of conditions over which, regardless of the value of uncertain parameters and the performance of the controllers, the process operation is safe, even due it may not be necessarily optimal.

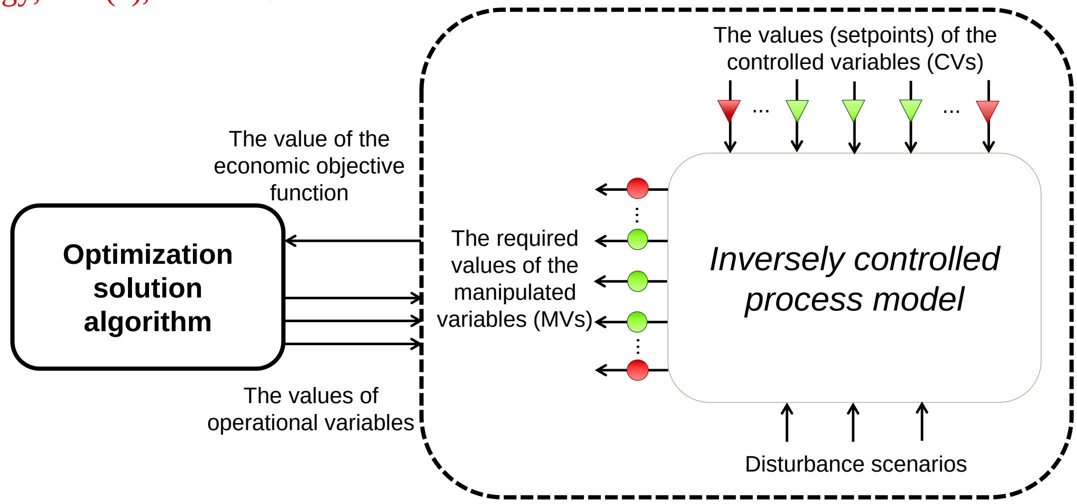

Fig. 2. Proposed optimization framework

3. Case study

In the present research, in order to demonstrate the application of the proposed optimization framework (Fig. 2), the integrated safe design and operation of an SOFC Triple Combined-cycle Power Generation System was studied. In the following first the process flow diagram is described. The optimization programming and implementation technique are presented and discussed.

3.1. SOFC Triple Combined-cycle Power Generation System: Process description

The process flow diagram of a SOFC Triple Combined-cycle Power Generation System is shown in Fig. 3 [1,58,59]. First, the natural gas and water are preheated in the economizers. Then, they are mixed and enter the reformer in order to produce the hydrogen-rich syngas stream. In addition, the combustion air is pressurized by the air compressor and preheated in an economizer. The hydrogen-rich syngas and air streams enter to the anode and cathode channels of the SOFC, respectively. The hydrogen in the syngas and the oxygen in the air react in the SOFC and produce steam and

Please cite this article at: Mahdi Sharifzadeh Mojtaba Meghdari, Davood Rashtchian. Multi-objective design and operation of Solid Oxide Fuel Cell (SOFC) Triple Combined-cycle Power Generation systems: Integrating energy efficiency and operational safety. Applied Energy, 185 (1), 345-361.

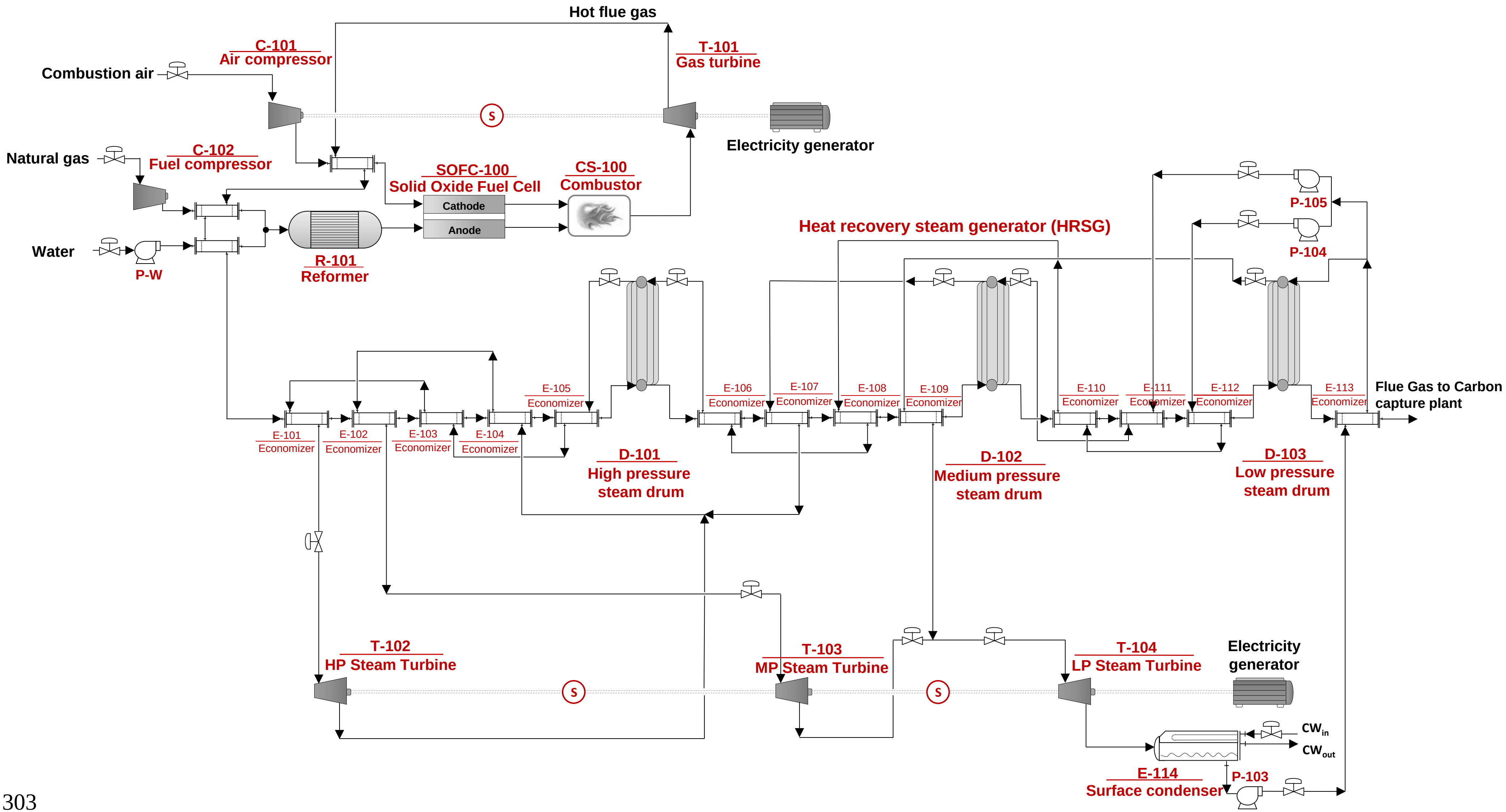

Fig. 3. The SOFC Triple Combined-cycle Power Generation System

Please cite this article at: Mahdi Sharifzadeh Mojtaba Meghdari, Davood Rashtchian. Multi-objective design and operation of Solid Oxide Fuel Cell (SOFC) Triple Combined-cycle Power Generation systems: Integrating energy efficiency and operational safety. Applied Energy, 185 (1), 345-361.

electricity. The direct current (DC) power produced in the SOFC stacks is converted to alternative current (AC) power via the DC/AC inverter, and sent to the electricity grid. The high temperature air stream from cathode channel and partially consumed syngas stream from the anode channel react in the combustion chamber. The hot flue gases are sent to the combined cycle gas turbine (CCGT) where their thermal energy is converted to electricity. A part of the generated electricity is used for driving the combustion air compressor. The exhaust gases exiting the gas turbine pass through the economizers to preheat air, water and natural gas feed streams. In addition, the temperature of the exhaust stream is sufficiently high to drive an additional bottoming steam cycle. Eventually, the exhaust gases are discharged to the atmosphere, or sent for CO_2 separation through a post-combustion carbon capture plant.

3.2. Optimization programming

This section described the optimization programming for integrated safe design and operation of an SOFC Triple Combined-cycle Power Generation System. The optimization technique adapted in the present research conforms to optimization with implicit constraints. The Genetic Algorithm (GA), a gradient-free optimization solution algorithm, was coupled with the Aspen Plus® Simulator. In the following, the multi-objective function, the optimization variables and the optimization constraints are discussed in more detail.

3.2.1. Multi-objective function

As discussed earlier, the multi-objective function consists of the economic and safety indicators.

$$\boldsymbol{F_{Total} = w_1 \times F_{Economic} + w_2 \times F_{Safety}} \qquad (\mathbf{1})$$

The solution of a multi-objective optimization is not a single solution but a Pareto front which demonstrate the trade-off between the competing objectives. Such a Pareto front can be constructed by changing the weighting factors $\boldsymbol{w_1}$ and $\boldsymbol{w_1}$ in equation (1). Both economic and safety objective were scaled, so they have the same order of magnitude. The weighting factors were varied between 0 and 1 in order to construct the Pareto front.

The economic measure was the total annual costs (TAC), defined as:

$$F_{Economic} = Capital\ investments/payback\ period\ + E(Operating\ Cost) \qquad (\mathbf{2})$$

The operating costs include the utility and feedstock costs and depend on the electricity load. Therefore, the expected value of operating costs is calculated according to the operating costs of various load scenarios and their likelihood.

$$E(Operating\ Cost) = \sum_{s=1}^{N_s} (L_s \times Operating\ Cost_s) \tag{3}$$

As discussed earlier, the aim of safety objective is to quantify the operating range over which safe operation of the process can be guaranteed:

$$F_{Safety} = E(Operating\ Cost) = \sum_{s=1}^{N_s} (L_s \times \delta_{i,s}) \tag{4}$$

In the above equation, $\delta_{i,s}$ were scaled according to the range of each manipulated variable and their average were applied as the objective function.

3.2.2. Optimization constraints

Optimization constraints can be classified into (1) first principles modelling constraints, (2) constraints associated with disturbance scenarios and uncertainties, (3) safety constraints and physical limitations, as discussed in the following.

3.2.2.1. First principles modelling constraints

The first principles modeling constraints refer to equality constraints concerning mass and energy balances, phase equilibrium and the performance curves of the process equipment such as the compressor and turbines. In the present research, the first principles model of the Triple Combined-cycle System power plant was developed in Aspen Plus® Simulation environment. The stream components were defined from the software databank. The Peng–Robinson property method was used for analysis. The model of conventional unit operations such as compressors, turbines, and heat exchangers were selected from the software model library. The reformer and combustion chamber were modelled based on chemical equilibrium, estimated by minimization of the Gibbs free energy. However, Aspen Plus® and associated Fortran Subroutines were found insufficient for accurate modelling of the solid oxide fuel cells (SOFCs). Therefore, the detailed model of the SOFC (according to [60]) was developed in MATLAB® and was exported to Aspen Plus®. The details of the SOFC model are reported in Supplementary Material (Table S2). It is notable that the SOFC model was initially developed in the COMSOL Multiphysics® (according to [61,62]) and was linked [63] to

MATLAB® according to the simulation-optimization shown in Fig. 4. However, synchronization of the three software (MATLAB®, Aspen Plus®, and COMSOL Multiphysics®) was found challenging and not practical for such a large-scale optimization problem. Therefore, the SOFC model was initially optimized in the MATLAB® environment and then the results were validated according to the more detailed model in COMSOL Multiphysics® (Fig. 7). The overall optimization framework is further discussed in Section 3.4.

3.2.2.2. Constraints associated with disturbance scenarios and uncertainties

Power generation systems are subject to variations in the electricity load, for example due to daily and hourly variations in the demand, or stochastic fluctuations such as extreme weather conditions. It is still expected to optimize the operating conditions in order to maximize the profit. Additional uncertainties can be caused by approximate estimation of model parameters or changes in the process behaviors over long operational periods. Examples of such uncertainties is the heat-transfer coefficients of the SOFC [64], where coke deposition results in significant variations of the system performance. In the present study, the scenarios corresponding to 100%, 75% and 50% electricity load of a 500 MW power plant were considered. In addition, +25% and -25% uncertainties in the SOFC heat-transfer coefficient were considered. The combination of these uncertainties results in nine disturbance scenarios (Shown in Table 1) that were considered for calculation of the aggregated objective functions. Without loss of generality, all scenarios and disturbances were considered equally likely.

As mentioned earlier, the disturbances are assumed equally likely, the average of the operating costs are considered. However, because equipment should remain operable for all disturbance scenarios, the process equipment was sized for the largest scenario, i.e., highest capital costs are considered. The costing correlations applied for calculating the objective function are listed in the Supplementary Materials (Table S1).

Table 1

Stochastic scenarios considered in the present study represent various combinations of uncertainties in the electricity loads and SOFC heat transfer coefficient.

Scenario	Change in the power demand (%)	Power demand (MW)	Changes in the heat transfer coefficient (%)	Heat transfer coefficient $W\ m^{-2}\ K^{-1}$
1st	0	500	-25	30
2nd	0	500	0	40
3th	0	500	+25	50
4th	-25	375	-25	30
5th	-25	375	0	40
6th	-25	375	+25	50
7th	-50	250	-25	30
8th	-50	250	0	40
9th	-50	250	+25	50

3.2.2.3. Safety constraints and physical limitations

As discussed earlier, the SOFC Triple Combined-Cycle Power Generation system utilizes a high degree of mass and energy integration. As a result, its operation is highly constrained by a variety of technical and safety measures. In the present research, the following safety constraints were included in the optimization program:

- Turbine inlet temperature must be maintained below $1550\,K$ in order to avoid thermal shock to process equipment [59,65,66].
- Similarly, throughout the SOFC stacks, the temperature must be maintained below $1400\,K$ in order to avoid thermal degradation [59,66].
- The surge margin (SM) of the compressors and turbines should be larger than 10% for safe operation [67].
- The steam to carbon ratio is maintained above $\lambda_{sc} > 2$ in order to avoid coke deposition [66].
- Too low fuel utilization (u_f) leads to low steam content in the anode recycle and high turbine inlet temperature and hence increases the risk of carbon deposition and compressor surge. Too high fuel utilization, on the other hand, leads to steep internal temperature gradients in the SOFC and therewith promotes thermal cracking. Therefore, the fuel utilization must be maintained in the range of 75-90% [59,66].
- The cell voltage must not drop under a certain level, as there is a maximum power output at an intermediate voltage. Lower voltage causes decreasing power in spite of increasing

current and is unfavorable. In the present research, a minimum voltage of 0.52 V was considered [66,68].

- The maximum cell current density that can be used to obtain a desired electrode reaction must be maintained below 5000 A/m^2 [59].

3.3. Optimization variables

As mentioned earlier, the optimization programming technique applied in the present study, conforms to optimization with implicit constraints, i.e. simulation-optimization. Therefore, the optimization variables which can be assigned independently are equivalent to the degree of freedom of the simulation program. They are listed in Table 2 and can be classified into process decision variables, and control decision variables. Process decision variables such as process configuration and the equipment size have physical realization. When the process is built, they are fixed and cannot be changed anymore. They for they are the same for all electricity load scenarios. However, control decision variables are available during the operational stages and can be adjusted in order to counteract or take advantage of the realization of uncertainties.

Table 2
Optimization variables: $\lambda_{SC,s}$ represents the ratio F_s^{Steam}/F_s^{Fuel} for disturbance scenario s. $\lambda_{Air,s}$ represents the ratio $F_s^{O_2}/F_s^{H_2}$ for disturbance scenario s.

Optimization variables	Description	Optimization variables	Description
N_{stacks}	Process decision variable	$F^{Fuel}_{Extreme\ Scenario,Down}$	Extreme MV
$F^{Fuel}_{s=1}$	Control decision variable	$\lambda^{SC}_{Extreme\ Scenario,Up}$	Extreme MV
$F^{Fuel}_{s=2}$	Control decision variable	$\lambda^{SC}_{Extreme\ Scenario,Down}$	Extreme MV
$F^{Fuel}_{s=3}$	Control decision variable	$\lambda^{Air}_{Extreme\ Scenario,Up}$	Extreme MV
$\lambda^{SC}_{s=1}$	Control decision variable	$\lambda^{Air}_{Extreme\ Scenario,Down}$	Extreme MV
$\lambda^{SC}_{s=2}$	Control decision variable	$\delta_{1,Fuel}$	
$\lambda^{SC}_{s=3}$	Control decision variable	$\delta_{2,Fuel}$	
$\lambda^{Air}_{s=1}$	Control decision variable	$\delta_{1,Steam}$	
$\lambda^{Air}_{s=2}$	Control decision variable	$\delta_{2,Steam}$	
$\lambda^{Air}_{s=3}$	Control decision variable	$\delta_{1,Air}$	
$F^{Fuel}_{Extreme\ Scenario,Up}$	Extreme MV	$\delta_{2,Air}$	

Note: MV refers to Manipulated variable

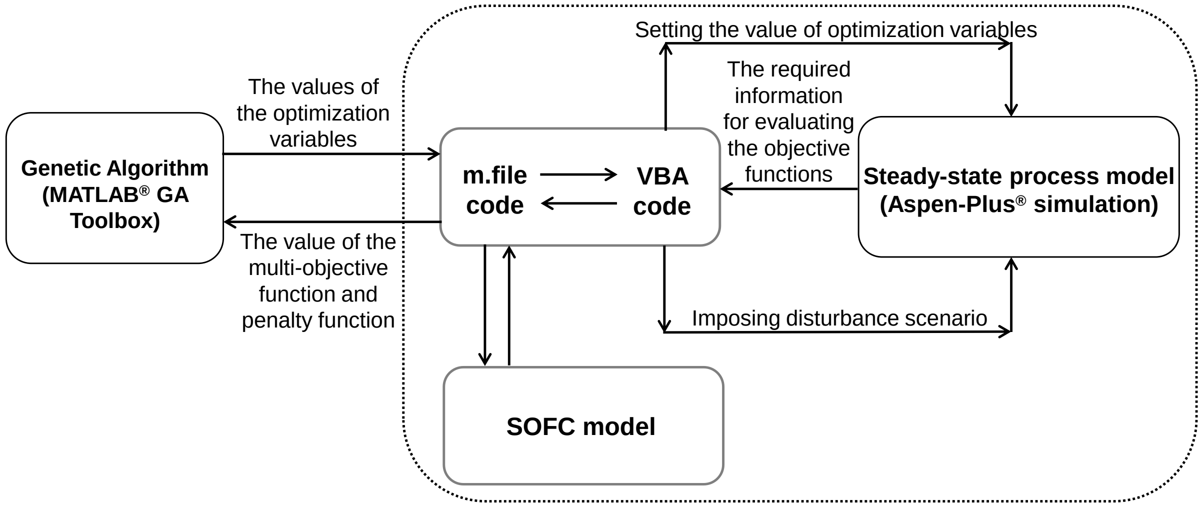

Fig. 4. Information flow of the simulation-optimization programming.

3.4. Implementation considerations

The simulation-optimization program for safe design and operation of the SOFC Triple Combined-Cycle Power generation system is shown in Fig. 4 and conforms to the framework of Fig. 2. The left envelope refers to the MATLAB® Genetic Algorithm. The right envelope represents the optimization constraints and consists of the codes in MATLAB® R2012a and Aspen Plus® V8.2. The main process diagram was modelled in Aspen Plus® [69]. However, as discussed earlier, the SOFC model was developed in MATLAB®. The SOFC model in Aspen Plus® Simulation was implemented as a user-defined unit operation and its performance was calculated and updated using the MATLAB® model. Unfortunately, due to technical difficulties, it was not possible to link MATLAB® directly to Aspen Plus®. Therefore, MATLAB® was firstly linked to Microsoft Excel/VBA® and then Microsoft Excel/VBA® was linked to Aspen Plus®. Integration was based on the Microsoft COM® automation interface.

While all the *Optimization Termination Criteria* are False, **Do**
- **Import** the *Optimization variables* (Equipment size, $y^{setpoint}$, $y^{extreme}$) from the *Genetic Algorithm*
- **For** each disturbance scenario, **Do**
  - **Set** the *Controlled variables* at their setpoints, $y^{setpoint}$
  - **Calculate** the *Operating Conditions* at the inlet of the SOFC in the Aspen Plus® simulation,
  - **Update** the MATLAB® SOFC model with the new operating conditions and **Run** the MATLAB® SOFC model.
  - **Calculate** the operating conditions at the outlet of the MATLAB® SOFC model and **Update** the Aspen Plus® Simulation.
  - **Run** the Aspen Plus® Simulation and **Record** the value of the required *Manipulated variable*, $u^{optimal}$,
  - **Calculate** *Economic Objective* function for the current disturbance scenario, $F_{Economic,s}$
  - **For** each safety constraint, **Do**
    - **Set** the *Controlled variables* to the current value of $y^{extreme}$
    - **Calculate** the *Operating Conditions* at the inlet of the SOFC using the Aspen Plus® simulation,
    - **Update** the MATLAB® SOFC model with the new operation conditions and **Run** the MATLAB® SOFC model.
    - **Calculate** the operating conditions at the outlet of the MATLAB® SOFC model and **Update** the Aspen Plus® Simulation.
    - **Run** the Aspen Plus® Simulation and **Record** the value of the Manipulated Variables at extreme, $u^{extreme}$
    - **Calculate** the *Safety Objective* function for the current safety constraint , $F_{Safety,s,extreme}$
  - **End For**
  - **Calculate** the *Safety Objective* function for the current disturbance scenario, $F_{saftey,s}$
- **End For**
- **Calculate** the aggregated *Economic Objective* function, $F_{Economic}$
- **Calculate** the aggregated *Safety Objective* function, F_{saftey}
- **Calculate** the value of aggregated total *Objective Function,* F_{Total} using the current value of weighting factors w_1 and w_2

End While

Fig. 5. The pseudocode for the simulation-optimization program applied for integrated safe design and operation of the Triple Combined-Cycle Power Generation system.

The main advantage of above-mentioned technique is the application of simulation software tools for accurate and convenient construction of large flow diagrams. However, since the optimization traverse a feasible path, it is necessary that the simulation program should converge in each optimization iteration. This is done by careful selection of the lower and upper bounds of the optimization variables. In addition, an error handler code was programed that systematically detect the failure of the simulation program and reinitialize the algorithm, if necessary. The default settings for the mutation, crossover and termination criteria were applied for the MATLAB® Generic Algorithm. The details of optimization software can be found in the MATLAB® documentations [70]. Fig. 5 shows the algorithm applied for implementation of the simulation-optimization framework. It consists of several nested loops of calculations. In each iteration of the optimization program, a simulation file was opened, run, and closed without saving. Since nine disturbance scenarios were considered, for each function recall the simulation was run nine times. The required time for each function recall was

6–7 min. Each generation of the optimization algorithm had fifty individuals, and the optimization needed at least twenty generations to converge. Considering different combination of weighting factors. In addition, in order to refine the penalty functions and scaling factors of the objectives, the optimization procedure needed to be reiterated a few times. As discussed earlier, the solution of a multi-objective optimization program forms a Pareto front which demonstrates the trade-off between the competing objectives. Based on the initial sensitivity analysis, nine combinations of weighting factors were considered which thoroughly covers the two extremes over which the economic and safety objectives are dominant. The optimization was defined as minimization of total annualized costs and unsafe operating range.

4. Results and discussions

This section presents and discusses the results of the optimization programming. The main feature of interest is the trade-off between the process profitability and the safe operating window. Such a trade-off is quantified using the Pareto fronts which represent the optimal solutions with various weights of the objective functions. Further discussions are enabled by investigating the details of process design and the changes in operational costs for various alternative designs, over a wide range of electricity power loads. The following discussions provide the proof of concept and a demonstrating example of how process design and safety objectives interact with each other and how to reach a desirable compromise between them.

4.1. Trade-off between process economy and safe operation

Fig. 6 shows the results of the multi-objective optimization for various combination of weighting factors. In this figure, W_9 refers to a design in which more emphasis is on the process flexibility and operational safety. By comparison, W_1 refers to an alternative design where the total annualized costs are minimized at the price of much narrower operating window. Fig 6.a suggests that expanding the safe operating window from 27.9% to 57.6% (almost 100%) would require 0.59×10^8 \$ year $^{-1}$ (i.e., 46.8%) increase in the total annualized costs. Fig. 6.b shows the variations of energy efficiency with the economic and safety objectives. These figures show that the economically competitive design which features high energy conversion efficiency, has a narrow safe operating window. Fig. 6.c- 6.f demonstrates how the costs of the SOFC stacks, compressors and turbines change as different weights are given to the safe operation objective. In all scenarios, expanding the safe operating window requires larger process equipment. For example, a larger number of SOFC stacks enables a larger flowrate of air with the cooling effect and therefore, such conservative design can handle larger variability in the fuel flowrate without violation of the maximum allowable temperature. Similarly, larger compressors and turbines can operate more flexibly without approaching the surge margins or chocking limits. Fig. 7 shows the range of safe operating window and the optimal operating points in the case of various electricity loads for three different weighting factors: $W_{Safety} = 10\%, 50\%\ and\ 90\%$. Fig. 7.a shows the range of fuel flow rates. As the electricity load decreases, the required fuel also decreases. However, for the processes with lower energy efficiency, larger flowrate is needed to meet the same electricity demand. Similar observation was made for steam feed (Fig. 7.b) to the reformer and the combustion air (Fig. 7.c), as they are proportional to the fuel flowrate. Fig. 8 shows the range of safe operating window and the optimal operating points of the combustion air compressor for the three weighting factors. They suggest that in order to expand the safe operating window, much larger compressor is needed, that implies much higher investment. Furthermore, as the safety weight increases, the operating point may not necessarily fall into the high energy efficiency regions.

Table 3
The optimal values of the optimization variables for different weighting factors of the safety objective

Optimization variables	Optimal value ($W_{Safety} = 10\%$)	Optimal value ($W_{Safety} = 50\%$)	Optimal value ($W_{Safety} = 90\%$)
N_{stacks}	5568	6316	7317
$F_{s=1}^{Fuel}$ $[kmol\ h^{-1}]$	2661.17	3145.91	3329.17
$F_{s=2}^{Fuel}$ $[kmol\ h^{-1}]$	2223.56	2385.6	2625.6
$F_{s=3}^{Fuel}$ $[kmol\ h^{-1}]$	1619.3	1653.3	1768.43
$F_{s=1}^{Steam}$ $[kmol\ h^{-1}]$	9209.69	11233.4	11613.3
$F_{s=2}^{Steam}$ $[kmol\ h^{-1}]$	7671.56	8373.78	8351.95
$F_{s=3}^{Steam}$ $[kmol\ h^{-1}]$	5673.94	5743.47	6073.5
$F_{s=1}^{Air}$ $[kg\ s^{-1}]$	850.88	1028.81	1132.95
$F_{s=2}^{Air}$ $[kg\ s^{-1}]$	726.47	781.72	813.66
$F_{s=3}^{Air}$ $[kg\ s^{-1}]$	526.14	537.5	566.57
$F_{Extreme\ Scenario,Up}^{Fuel}$ $[kmol\ h^{-1}]$	2718.17	3390.69	3850.06
$F_{Extreme\ Scenario,Down}^{Fuel}$ $[kmol\ h^{-1}]$	1172.51	1104.25	997.25
$F_{Extreme\ Scenario,Up}^{Steam}$ $[kmol\ h^{-1}]$	9199.31	12570.4	14369.65
$F_{Extreme\ Scenario,Down}^{Steam}$ $[kmol\ h^{-1}]$	3279.24	3088.33	2589.63
$F_{Extreme\ Scenario,Up}^{Air}$ $[kg\ s^{-1}]$	889.92	1182.13	1439.55
$F_{Extreme\ Scenario,Down}^{Air}$ $[kg\ s^{-1}]$	305.7	283.01	242.16
$\delta'_{1,Fuel}$ $[\%]$	1.9	8.16	17.38
$\delta'_{2,Fuel}$ $[\%]$	13.89	18.30	25.71
$\delta'_{1,Steam}$ $[\%]$	1.18	8.35	17.22
$\delta'_{2,Steam}$ $[\%]$	14.03	16.58	21.77
$\delta'_{1,Air}$ $[\%]$	2.04	10.03	23.13
$\delta'_{2,Air}$ $[\%]$	12.92	15.62	19.92

Table 3 shows the optimal values of the decision variables for different weighting factors of the safety objective. The features of interest include the number of SOFC stacks, the nominal and part load operating points of the turbines and compressors, the flowrate of natural gas fuel, combustion air and steam for each scenario, the length of the safe operating window. These results are visualized and further discussed in the following sections.

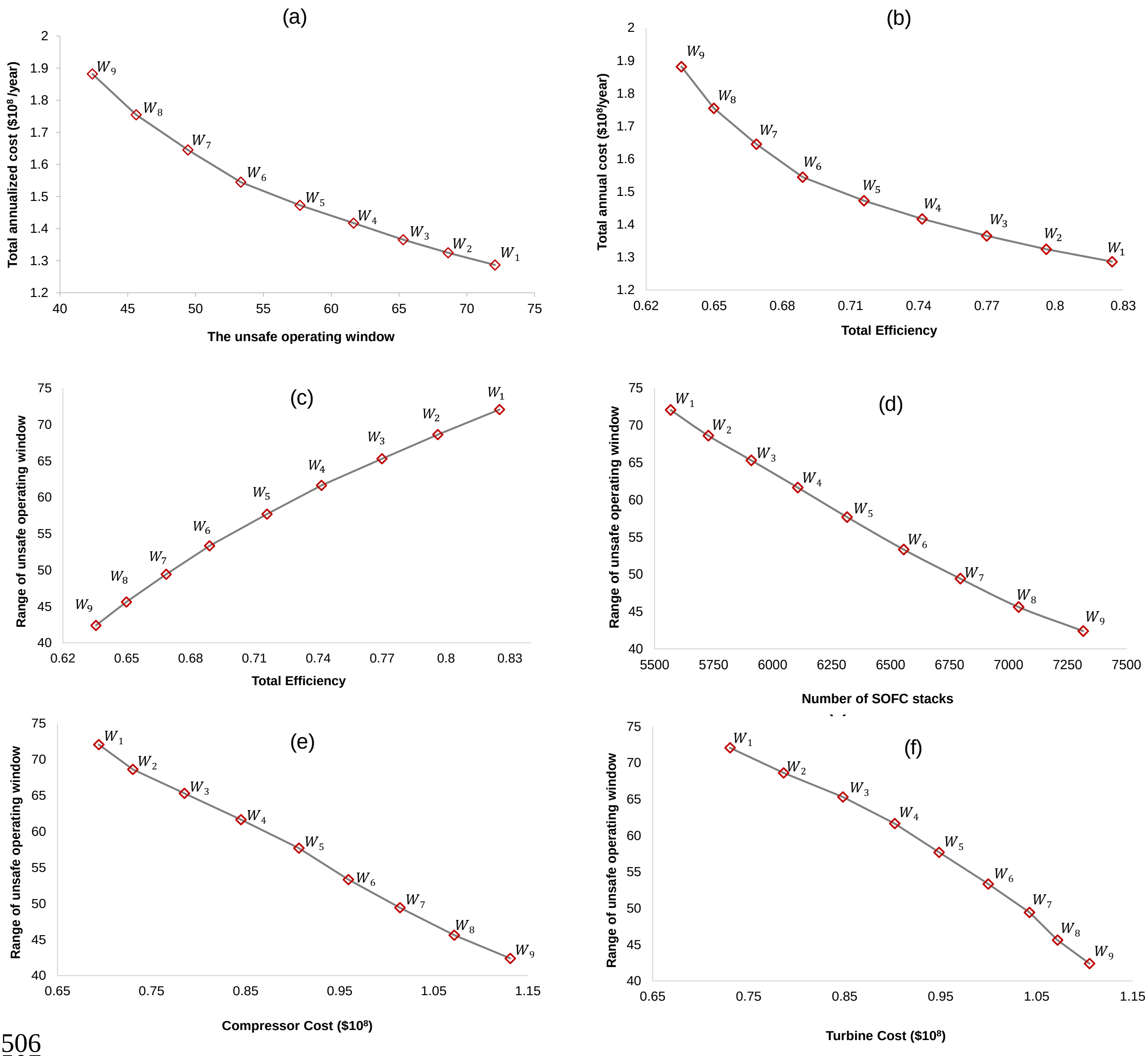

Fig. 6. (a) The Pareto Front demonstrating the trade-off between the process economy and safe operating window, **(b)** Total annual costs versus average efficiency for all scenario, **(c)** The range of unsafe operating window versus average efficiency for all scenario, **(d)** The trade-off between the range of unsafe operating window and the number of SOFC stacks. **(e)** The trade-off between the range of unsafe operating window and the compressor cost, **(f)** The trade-off between the range of unsafe operating window and the gas turbine cost.

Please cite this article at: Mahdi Sharifzadeh Mojtaba Meghdari, Davood Rashtchian. Multi-objective design and operation of Solid Oxide Fuel Cell (SOFC) Triple Combined-cycle Power Generation systems: Integrating energy efficiency and operational safety. Applied Energy, 185 (1), 345-361.

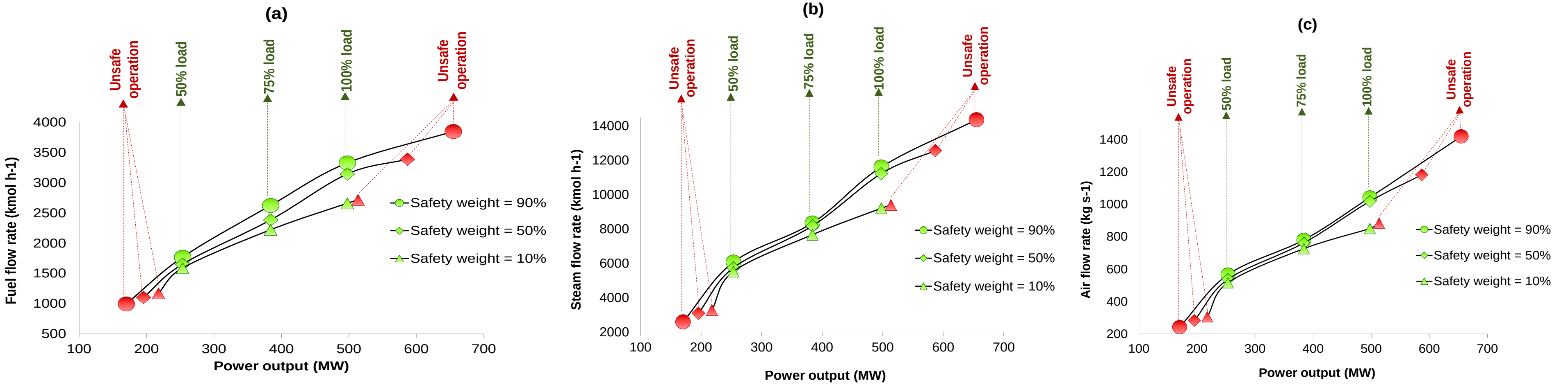

Fig. 7. (a) The safe range of fuel flow rate. (b) The safe range of steam flow rate. (c) The safe range of Air flow rate.

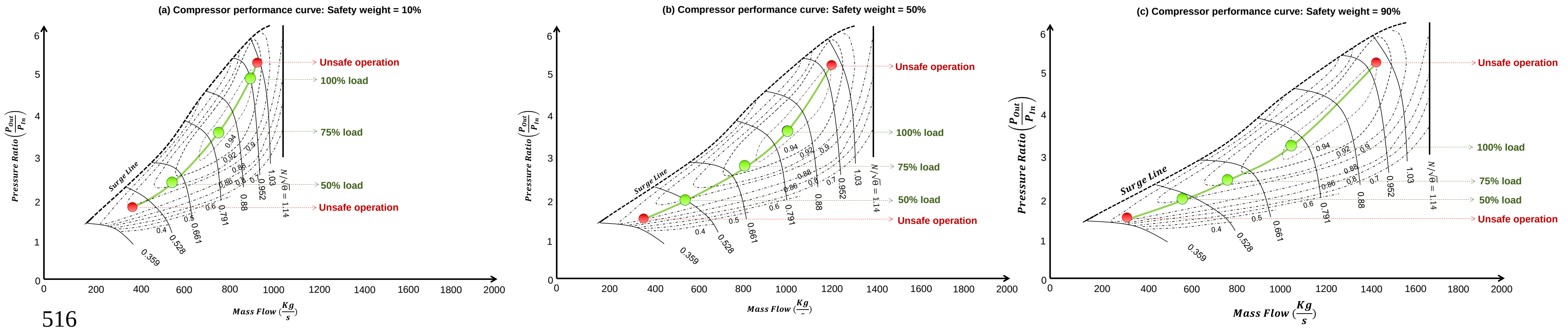

Fig. 8. The safe range of air flow rate: (a) $W_{Safety} = 10\%$, (b) $W_{Safety} = 50\%$ and (c) $W_{Safety} = 90\%$.

4.2. Validation of the results using full physics model.

The details of SOFC operation are shown in Figs. 9 and 10. Fig 9 shows the temperature profiles for seven segments of the fuels cell: the fuel channel and anode electrode on the left, the air channel and cathode electrode on the right, and the Electrolyte in the middle. The figures arranged in columns refer to different weighting factors, $\boldsymbol{w_1} = 0.1, 0.5, 0.9$. The red color in Fig. 9 represents extremely high temperatures. In the present research, the temperature above 1400K are considered to be unsafe and detrimental to the equipment. The figures arranged in rows have similar power load (50%, 75% and 100%). The figures arranged in columns have similar safety weight on the design of the fuel cells. The top rows show that for part loads (e.g., 50%), the temperature profile is well below 1350K and away from unsafe operational threshold. However, as the flowrate of syngas and air increases, the temperature of both left and right channels increases until they reach the maximum allowable temperature (1400K). The figures arranged in columns shows the implication of the safety weight on the design of the fuel cells. As mentioned earlier, the fuel cells were modular and the optimization program had the option to increase the number of the fuel cell stacks. Fig. 9 illustrates that as the safety weighting factor increases, the optimization chooses a larger number of Fuel Cells for further distribution of the syngas and mitigation of the risk of hot spots.

Fig. 10 provides additional results in terms of the compositions of the hydrogen and oxygen in the anode and cathode, for the same scenarios. These figures show that in part load scenarios, the mole fraction of hydrogen is relatively high throughout the anode channel. However, as the electricity load increases, the rate of the reactions also increases and hydrogen concentration depletes sharply at the fuel cell exit.

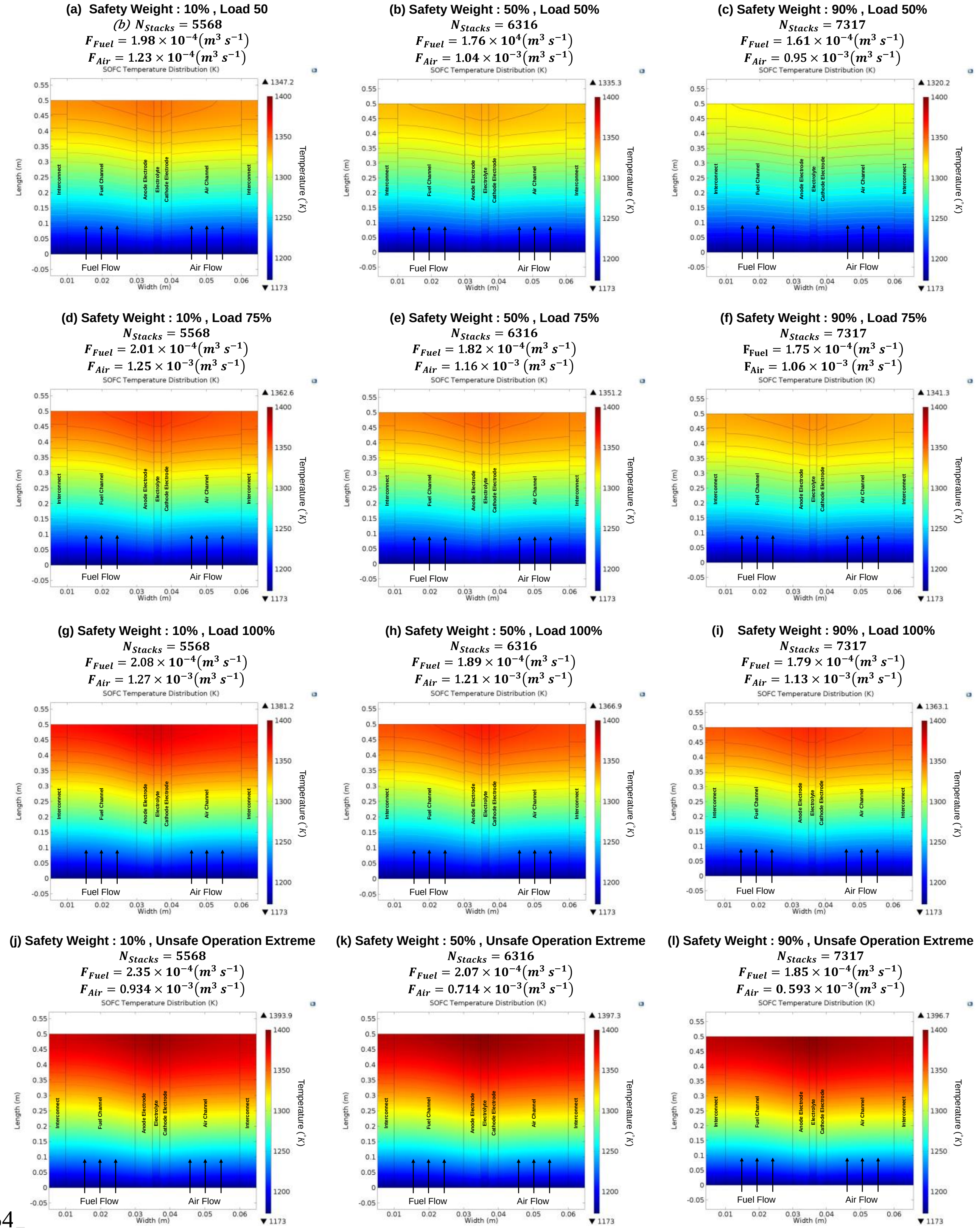

Fig. 9. The temperature profiles for various safety weighting factors (columns) and power loads (rows). The total number of fuel cell stacks and the flowrate of each channel is shown on each figure.

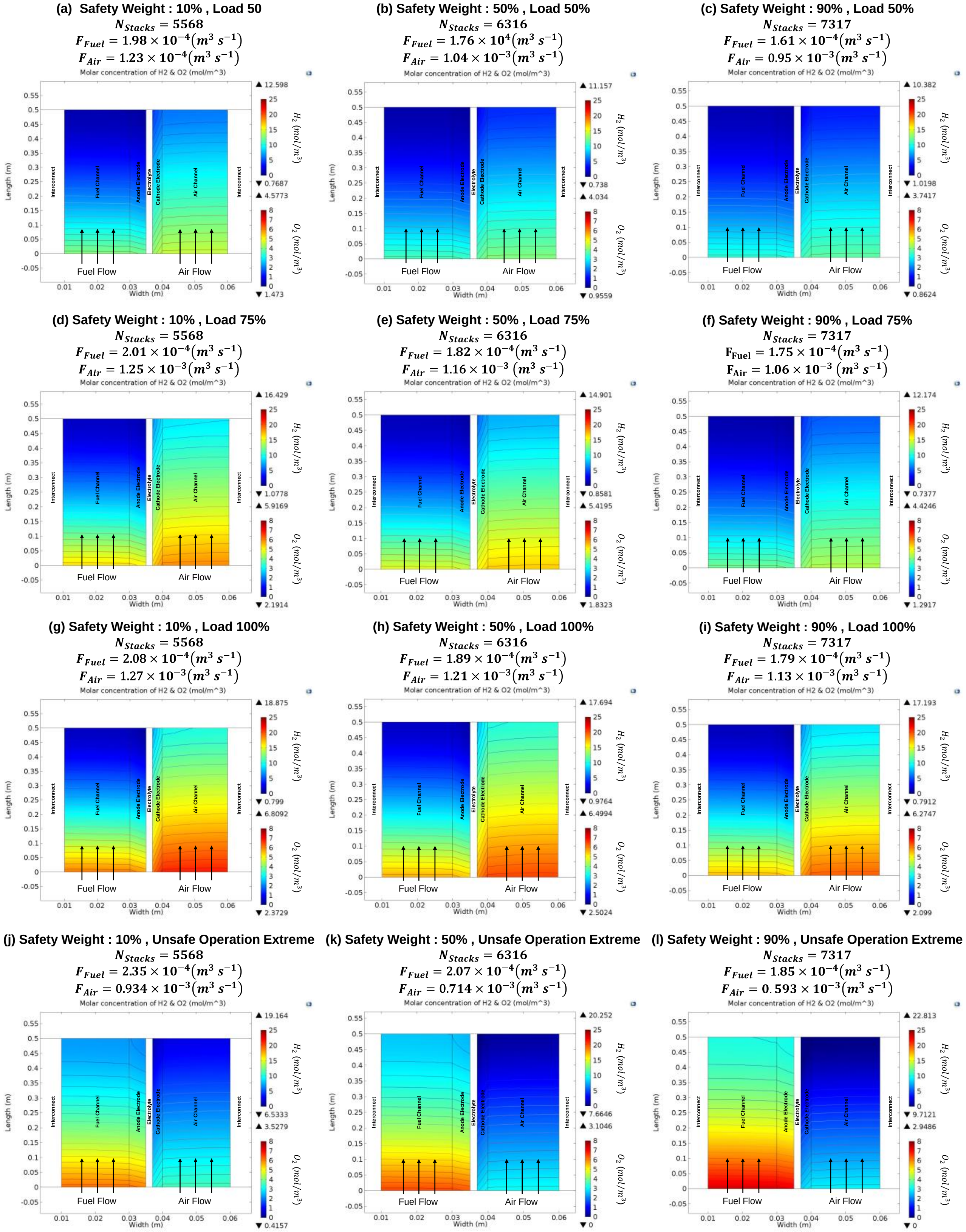

Fig. 10. The compositions of hydrogen and oxygen for various safety weighting factors (columns) and electricity power loads (rows). The total number of fuel cell stacks and the flowrate of each channel is shown on each figure.

4.3. The implications of safe design and operation for the exergy flows

The last part of post-optimization analysis investigates the exergy flows across the process components. As discussed earlier, the proposed multi-objective optimization framework quantified the energetic performance in economic terms. The aim of this section is to quantify the overall energetic performance and underpin key energy consumers for various design scenarios and under variable electricity loads. This will illustrate how the trade-offs between economic and safety measures alters the energy distribution across the solid oxide fuel cell (SOFC) triple combined-cycle power generation system.

Fig. 11 shows the results of exergy analysis, which conform to the flow diagram in Fig. 3. The thickness of each stream corresponds to the exergy flow of that stream. The numerical values of the exergy flows are also indicated. The comparison is between the exergy flows for different safety weights (row) for various electricity loads (Columns). As shown in the top row of Fig. 11, the overall exergetic efficiency of the safest plant (Safety weight 90%) is about 67% and 60% for maximum and minimum loads, respectively. By comparison, in the bottom row, when a higher weight is given to the economic objective function (Safety weight 10%), the overall exergetic efficiency increases to 71% and 64% for maximum and minimum loads, respectively. In the design with 90% safety factor, 251.4 MW is generated in the Gas Turbine and 107.2 MW is generated in the SOFC stacks. By comparison in the design with 10% safety factor, 372.2 MW is generated in the Gas Turbine and 83.2 MW was the contribution of the SOFC. The key observation is that when the process is designed for the higher weight of safety, the optimizer chooses to allocate more power generation to the SOFC stacks. However, when the economic objective is dominant, the power is more generated in the gas turbine. Similar results were observed for the electricity loads of 75% and 50%.

Fig. 12 shows the exergy destruction distribution in each unit of the power plant. The results show that the SOFC stack, afterburner and heat recovery/ steam generation system (HRSG) are responsible for the major exergy destruction in the system, they are responsible for approximately 80% of the overall exergy destruction. Similar results were reported by other researchers [13,21]. As shown in Fig. 12, the exergy destruction of SOFC stack, Afterburner and HRSG & ST system in safety weight 90% is greater than those of safety weight 50% and 10%, and the exergy destruction rate of SOFC stack for all scenarios is above 30%. The plant overall exergetic efficiency of the safest plant (Safety weight

Please cite this article at: Mahdi Sharifzadeh Mojtaba Meghdari, Davood Rashtchian. Multi-objective design and operation of Solid Oxide Fuel Cell (SOFC) Triple Combined-cycle Power Generation systems: Integrating energy efficiency and operational safety. Applied Energy, 185 (1), 345-361.

90%) is about 67% and 60% for maximum and minimum load, respectively. The plant overall exergetic efficiency of most economic plant (Safety weight 10%) is about 71% and 64% for maximum and minimum load, respectively.

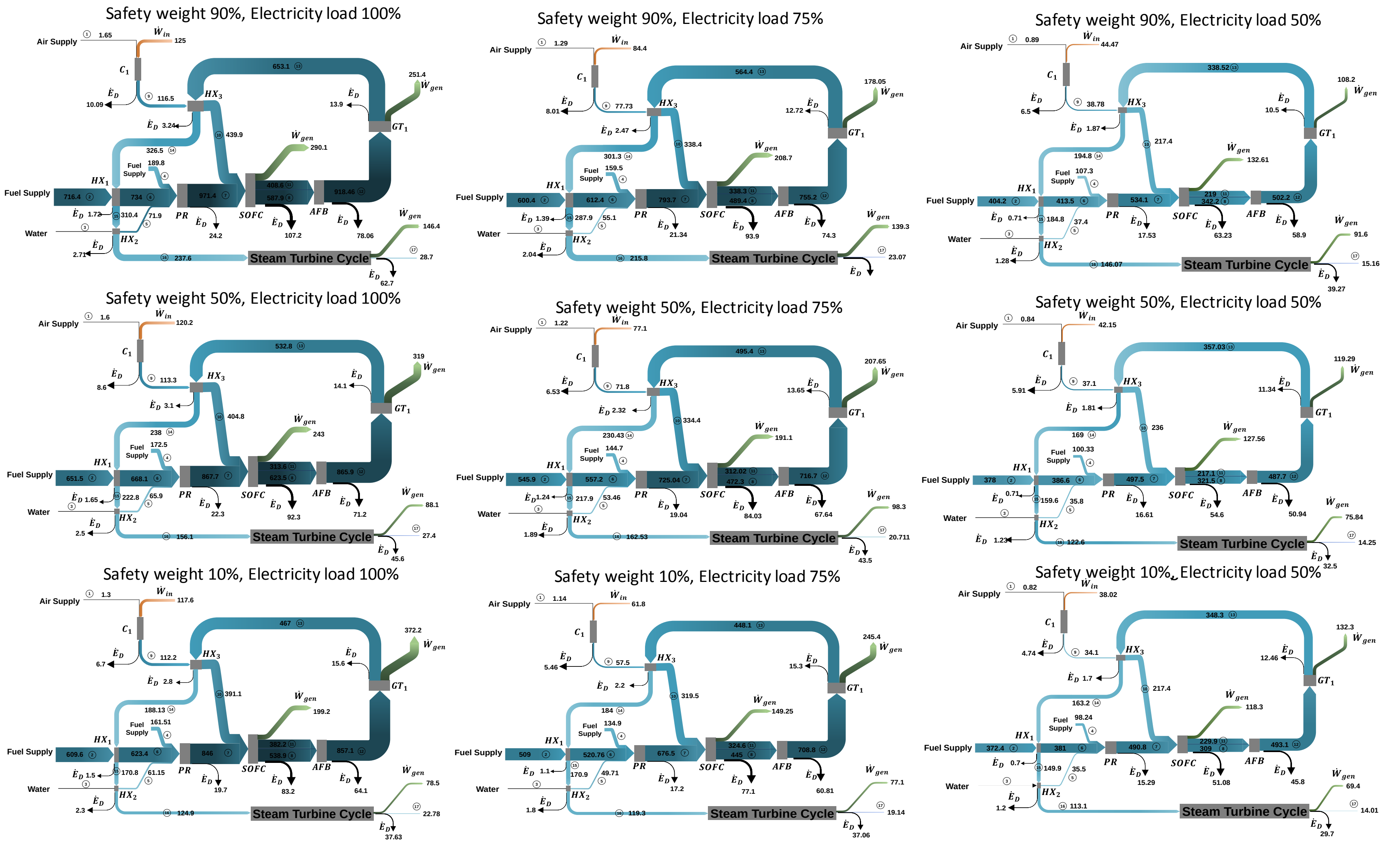

Fig. 11. (a) Sankey diagram for various safety weights (100% electricity load); (b) Sankey diagram for various safety weights (75% electricity load), (c) Sankey diagram for various safety weights (50% electricity load)

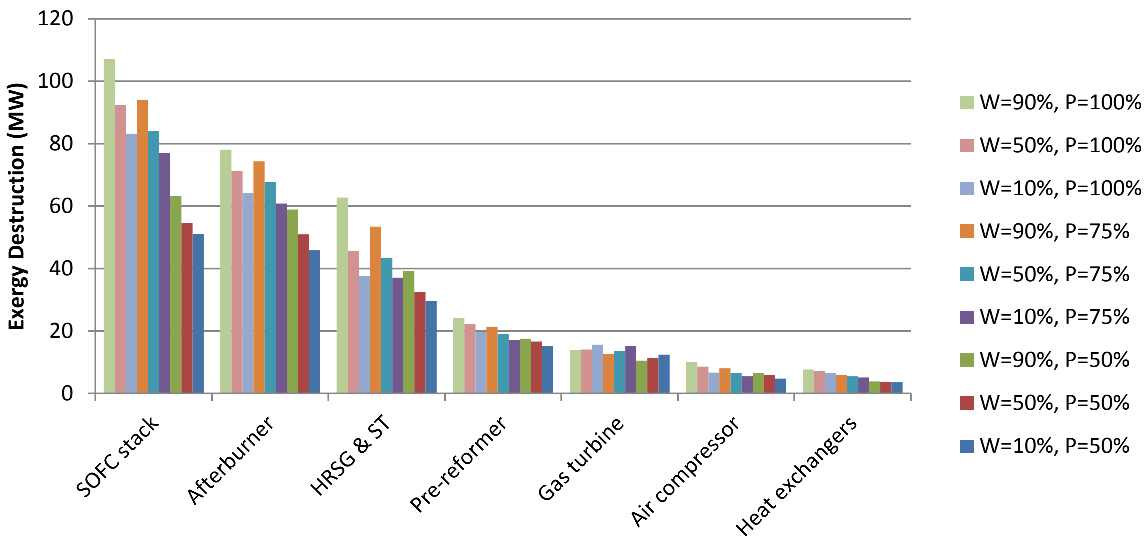

Fig. 12. The exergy destruction distributions of various unit operation, different electricity load and different safety weight in the multi-objective function

5. Conclusion

Process industries are associated with hazardous chemicals and extreme operating conditions. Unsafe events can incur dramatic costs in terms of the loss of life, financial penalties and damages to the environment. Industrial processes must be safely operable over a wide range of operating conditions. Nevertheless, operation of industrial processes is a strong function of their design. If the process is initially poorly designed, ensuring its safe operation, if not impossible, would require costly modifications, and production interruptions at the operational phases. Therefore, many commentators recommended that the design and operation of industrial processes should be considered simultaneously. The challenge is that during the process design phase, there are large uncertainties in the operational conditions. In the present research, a novel framework was developed that ensures the process safe operation and simultaneously optimizes other design objectives such as process profitability in the presence of uncertainties. The research methodology was demonstrated on the case of a Solid Oxide Fuel Cell (SOFC) Triple Combined-cycle System. The significance of this industrial application is that while SOFC power plants apply a high degree of mass and heat integration, resulting in very narrow operating window, they are also subject to significant uncertainties in electricity power load. Furthermore, their behavior may change over the time, for instance, due to coking in the fuel cells.

The key findings of the present research include:

- ✓ There is a strong trade-off between the profitability and the range of safe operating window. It was observed that highly economic designs have much narrower operating window.
- ✓ The violation of safety constraints such as maximum allowable temperature in the SOFC and gas turbine inlet temperature impose strong limits on the operating conditions and process economy.
- ✓ The results of exergy analysis reveals that the balance between the power generated in the SOFC and gas turbine was the key decision to establish the length of the operating window.

The results of the case study demonstrated a strong trade-off between the range of safe process operation and the process economy in terms of the required capital investment and operating costs. Furthermore, it was shown that it is possible to establish the trade-off, so the process profitability is maximized and at the same time the process safe operation is ensured in the presence of the uncertainties. While these results provide the proof of concept, they are to large extent general and expected to be transferable to other industrial processes.

The present study demonstrated the strong trade-off between the energetic performance (quantified in economic terms) and operational safety. Nonetheless, there are other competing objectives such as environmental indicators that could be included in the formulation. We will consider this aspect in our future studies.

In the present research steady-state process model was applied for identifying the process operability before and after disturbances. However steady-state formulations do not have any implications for the transient states between initial and final process conditions. For the industrial processes with highly dynamic behavior, or those with the risk of violating path constraints, the proposed optimization framework should be formulated in dynamic terms (similar to work of [55]). While, solving large-scale dynamic optimization problems is a tough challenge for current optimization technology, developing tailor-made optimization algorithms will remain a frontier in research.

References

[1] Buonomano A, Calise F, d'Accadia MD, Palombo A, Vicidomini M. Hybrid solid oxide fuel cells-gas turbine systems for combined heat and power: A review. Appl Energy 2015;156:32–85.

[2] Yi Y, Rao AD, Brouwer J, Samuelsen GS. Analysis and optimization of a solid oxide fuel cell and intercooled gas turbine (SOFC-ICGT) hybrid cycle. J Power Sources 2004;132:77–85.

[3] McLarty D, Brouwer J, Samuelsen S. Fuel cell-gas turbine hybrid system design part I: Steady state performance. J Power Sources 2014;257:412–20.

[4] Sharifzadeh M, Shah N. Carbon capture from natural gas combined cycle power plants: Solvent performance comparison at an industrial scale. AIChE J 2016;62:166–79.

[5] Sharifzadeh M, Bumb P, Shah N. Carbon capture from pulverized coal power plant (PCPP): Solvent performance comparison at an industrial scale. Appl Energy 2016;163:423–35.

[6] Sucipta M, Kimijima S, Suzuki K. Performance analysis of the SOFC-MGT hybrid system with gasified biomass fuel. J Power Sources 2007;174:124–35.

[7] Curletti F, Gandiglio M, Lanzini A, Santarelli M, Maréchal F. Large size biogas-fed Solid Oxide Fuel Cell power plants with carbon dioxide management: Technical and economic optimization. J Power Sources 2015;294:669–90.

[8] Hou X, Marin-Flores O, Kwon BW, Kim J, Norton MG, Ha S. Gasoline-fueled solid oxide fuel cell with high power density. J Power Sources 2014;268:546–9.

[9] Nease J, Adams TA. Coal-fuelled systems for peaking power with 100% CO2 capture through integration of solid oxide fuel cells with compressed air energy storage. J Power Sources 2014;251:92–107.

[10] Cinti G, Desideri U. SOFC fuelled with reformed urea. Appl Energy 2015;154:242–53.

[11] Andersson M, Yuan J, Sundén B. Review on modeling development for multiscale chemical reactions coupled transport phenomena in solid oxide fuel cells. Appl Energy 2010;87:1461–76.

[12] Zhao Y, Sadhukhan J, Lanzini A, Brandon N, Shah N. Optimal integration strategies for a syngas fuelled SOFC and gas turbine hybrid. J Power Sources 2011;196:9516–27.

[13] Calise F, Palombo A, Vanoli L. Design and partial load exergy analysis of hybrid SOFC-GT power plant. J Power Sources 2006;158:225–44.

[14] Zhang X, Chan SH, Li G, Ho HK, Li J, Feng Z. A review of integration strategies for solid oxide fuel cells. J Power Sources 2010;195:685–702.

[15] Cheddie DF, Murray R. Thermo-economic modeling of an indirectly coupled solid oxide fuel cell/gas turbine hybrid power plant. J Power Sources 2010;195:8134–40.

[16] Arsalis A. Thermoeconomic modeling and parametric study of hybrid SOFC-gas turbine-steam turbine power plants ranging from 1.5 to 10 MWe. J Power Sources 2008;181:313–26.

[17] Zaccaria V, Tucker D, Traverso A. Transfer function development for SOFC/GT hybrid systems control using cold air bypass. Appl Energy 2016;165:695–706.

[18] Harun NF, Tucker D, II TAA. Impact of fuel composition transients on SOFC performance in gas turbine hybrid systems. Appl Energy 2016;164:446–61.

[19] Fardadi M, McLarty DF, Jabbari F. Investigation of thermal control for different SOFC flow geometries. Appl Energy 2016;178:43–55.

[20] Facci AL, Cigolotti V, Jannelli E, Ubertini S. Technical and economic assessment of a SOFC-based energy system for combined cooling, heating and power. Appl Energy 2016.

[21] Varga T, Horváth G, Abonyi J. Determination of Safety Operating Regimes Based on the Analysis of Characteristic Equation of State-Space Model. Hungarian J Ind Chem 2008;36:149–53.

[22] Rusli R, Mohd Shariff A. Qualitative Assessment for Inherently Safer Design (QAISD) at preliminary design stage. J Loss Prev Process Ind 2010;23:157–65.

[23] Huang H, Adjiman CS, Shah N. Quantitative framework for reliable safety analysis. AIChE J 2002;48:78–96.

[24] Shariff AM, Zaini D. Toxic release consequence analysis tool (TORCAT) for inherently safer design plant. J Hazard Mater 2010;182:394–402.

[25] Marhavilas PK, Koulouriotis D, Gemeni V. Risk analysis and assessment

methodologies in the work sites: On a review, classification and comparative study of the scientific literature of the period 2000-2009. J Loss Prev Process Ind 2011;24:477–523.

[26] Nolan DP. Applications of HAZOP and What-If Safety Reviews to the Petroleum, Petrochemical and Chemical Industries. William Andrew; 1995.

[27] Kim J, Lee Y, Moon I. An index-based risk assessment model for hydrogen infrastructure. Int J Hydrogen Energy 2011;36:6387–98.

[28] Groso A, Ouedraogo A, Meyer T. Risk analysis in research environment. J Risk Res 2012;15:187–208.

[29] Raspotnig C, Opdahl A. Comparing risk identification techniques for safety and security requirements. J. Syst. Softw., vol. 86, 2013, p. 1124–51.

[30] Suardin J, Sam Mannan M, El-Halwagi M. The integration of Dow's fire and explosion index (F&EI) into process design and optimization to achieve inherently safer design. J Loss Prev Process Ind 2007;20:79–90.

[31] Khan FI, Amyotte PR. I2SI: A comprehensive quantitative tool for inherent safety and cost evaluation. J. Loss Prev. Process Ind., vol. 18, 2005, p. 310–26.

[32] Leong CT, Shariff AM. Process route index (PRI) to assess level of explosiveness for inherent safety quantification. J Loss Prev Process Ind 2009;22:216–21.

[33] Srinivasan R, Nhan NT. A statistical approach for evaluating inherent benign-ness of chemical process routes in early design stages. Process Saf Environ Prot 2008;86:163–74.

[34] Ahmad SI, Hashim H, Hassim MH. Numerical Descriptive Inherent Safety Technique (NuDIST) for inherent safety assessment in petrochemical industry. Process Saf Environ Prot 2014;92:379–89.

[35] Leong CT, Shariff AM. Inherent safety index module (ISIM) to assess inherent safety level during preliminary design stage. Process Saf Environ Prot 2008;86:113–9.

[36] Gangadharan P, Zanwar A, Zheng K, Gossage J, Lou HH. Sustainability assessment of polygeneration processes based on syngas derived from coal and natural gas. Comput Chem Eng 2012;39:105–17.

[37] Medina-Herrera N, Jimenez-Gutierrez A, Mannan MS. Development of inherently safer distillation systems. J Loss Prev Process Ind 2014;29:225–39.

[38] Tugnoli A, Khan F, Amyotte P, Cozzani V. Safety assessment in plant layout design using indexing approach: Implementing inherent safety perspective. Part 1 - Guideword applicability and method description. J Hazard Mater 2008;160:100–9.

[39] Tugnoli A, Khan F, Amyotte P, Cozzani V. Safety assessment in plant layout design using indexing approach: Implementing inherent safety perspective: Part 2—Domino Hazard Index and case study. J Hazard Mater 2008;160:110–21.

[40] Di Domenico J, Vaz CA, de Souza MB. Quantitative risk assessment integrated with process simulator for a new technology of methanol production plant using recycled CO2. J Hazard Mater 2014;274:164–72.

[41] Koc R, Kazantzis NK, Nuttall WJ, Ma YH. Economic assessment of inherently safe membrane reactor technology options integrated into IGCC power plants. Process Saf Environ Prot 2012;90:436–50.

[42] Meel A, Seider WD. Real-time risk analysis of safety systems. Comput Chem Eng 2008;32:827–40.

[43] Podofillini L, Dang VN. Conventional and dynamic safety analysis: Comparison on a chemical batch reactor. Reliab Eng Syst Saf 2012;106:146–59.

[44] Yang SH, Yang L, He CH. Improve Safety of Industrial Processes Using Dynamic Operator Training Simulators. Process Saf Environ Prot 2001;79:329–38.

[45] Maria G, Stefan DN. Variability of operating safety limits with catalyst within a fixed-bed catalytic reactor for vapour-phase nitrobenzene hydrogenation. J Loss Prev Process Ind 2010;23:112–26.

[46] Dimitriadis VD, Hackenberg J, Shah N, Pantelides CC. A case study in hybrid process

safety verification. Comput Chem Eng 1996;20:S503–8.

[47] Lin Y, Stadtherr MA. Rigorous model-based safety analysis for nonlinear continuous-time systems. Comput Chem Eng 2009;33:493–502.

[48] Uygun K, Huang Y, Lou HH. Fast process security assessment theory. AIChE J 2004;50:2187–202.

[49] Eini S, Shahhosseini HR, Javidi M, Sharifzadeh M, Rashtchian D. Inherently safe and economically optimal design using multi-objective optimization: The case of a refrigeration cycle. Process Saf Environ Prot 2016;104.

[50] Shah NM, Hoadley AFA, Rangaiah GP. Inherent Safety Analysis of a Propane Precooled Gas-Phase Liquified Natural Gas Process. Ind Eng Chem Res 2009;48:4917–27.

[51] El-Halwagi AM, Rosas C, Ponce-Ortega JM, Jim??nez-Guti??rrez A, Mannan MS, El-Halwagi MM. Multiobjective optimization of biorefineries with economic and safety objectives. AIChE J 2013;59:2427–34.

[52] Sharifzadeh M. Integration of process design and control: A review. Chem Eng Res Des 2013;91:2515–49.

[53] Sharifzadeh M, Thornhill NF. Optimal selection of control structure using a steady-state inversely controlled process model. Comput Chem Eng 2012;38:126–38.

[54] Sharifzadeh M. Implementation of a steady-state inversely controlled process model for integrated design and control of an ETBE reactive distillation. Chem Eng Sci 2013;92:21–39.

[55] Sharifzadeh M, Thornhill NF. Integrated design and control using a dynamic inversely controlled process model. Comput Chem Eng 2013;48:121–34.

[56] Grossmann IE, Calfa BA, Garcia-Herreros P. Evolution of concepts and models for quantifying resiliency and flexibility of chemical processes. Comput Chem Eng 2014;70:22–34.

[57] Grossmann IE, Halemane KP, Swaney RE. Optimization strategies for flexible chemical processes. Comput Chem Eng 1983;7:439–62.

[58] Lv X, Lu C, Wang Y, Weng Y. Effect of operating parameters on a hybrid system of intermediate-temperature solid oxide fuel cell and gas turbine. Energy 2015;91:10–9.

[59] Shirazi A, Aminyavari M, Najafi B, Rinaldi F, Razaghi M. Thermal-economic-environmental analysis and multi-objective optimization of an internal-reforming solid oxide fuel cell-gas turbine hybrid system. Int J Hydrogen Energy 2012;37:19111–24.

[60] Bavarian M, Soroush M. Steady-state multiplicity in a solid oxide fuel cell: Practical considerations. Chem Eng Sci 2012;67:2–14.

[61] Tseronis K, Bonis I, Kookos IK, Theodoropoulos C. Parametric and transient analysis of non-isothermal, planar solid oxide fuel cells. Int J Hydrogen Energy 2012;37:530–47.

[62] Serincan MF, Pasaogullari U, Sammes NM. Effects of operating conditions on the performance of a micro-tubular solid oxide fuel cell (SOFC). J Power Sources 2009;192:414–22.

[63] Sharifzadeh M, Rashtchian D, Pishvaie MR, Thornhill NF. Energy induced separation network synthesis of an olefin compression section: A case study. Ind Eng Chem Res 2011;50.

[64] Mangold M, Krasnyk M, Sundmacher K. Theoretical investigation of steady state multiplicities in solid oxide fuel cells. J Appl Electrochem 2006;36:265–75.

[65] Wächter C, Lunderstädt R, Joos F. Using Linear Control Theory for Parameterization of a Controller for a SOFC/GT Hybrid Power Plant. J Fuel Cell Sci Technol 2010;7:31003-1-031003–9.

[66] Wu X-J, Zhu X-J. Optimization of a solid oxide fuel cell and micro gas turbine hybrid system. Int J Energy Res 2013;37:242–9.

[67] Jia Z, Sun J, Dobbs H, King J. Feasibility study of solid oxide fuel cell engines integrated with sprinter gas turbines: Modeling, design and control. J Power Sources

2015;275:111–25.

[68] Stiller C, Thorud B, Bolland O, Kandepu R, Imsland L. Control strategy for a solid oxide fuel cell and gas turbine hybrid system. J Power Sources 2006;158:303–15.

[69] Aspen Technology. Aspen Plus ® User Guide. Aspen Technol Inc 2000:936.

[70] MATLAB® Documentation, Optimization Toolbox User's Guide. Mathworks 2016. http://www.mathworks.co.uk/help/pdf_doc/optim/optim_tb.pdf (accessed September 1, 2016).